

# Phase contrast techniques for wavefront sensing and calibration in adaptive optics

E. E. Bloemhof and J. K. Wallace  
Jet Propulsion Laboratory, California Institute of Technology,  
Pasadena, CA USA 91109

## ABSTRACT

The wavefront sensor is the most critical component of an adaptive optics (AO) system. Most astronomical systems use one of a small number of alternatives, notably the Shack-Hartmann or the curvature sensor; these are sensitive to the first and second derivative of the wavefront phase, respectively. In this paper, we explore a novel adaptation of the phase-contrast technique developed for microscopy by Zernike to measure phase directly, and show that it is potentially useful in astronomical adaptive optics, both for closed-loop wavefront sensing and for off-line calibration of the system PSF. The phase-contrast WFS should enjoy an advantage in lower read noise, as well as a natural match to the piston-type deformable mirror actuators commonly in use with most current Shack-Hartmann systems, and favorable error propagation during wavefront reconstruction. It appears that it might be possible to implement versions with the reasonably broad spectral bandwidth desired for astronomical applications, and to integrate them with relatively minor modifications to existing AO system architectures.

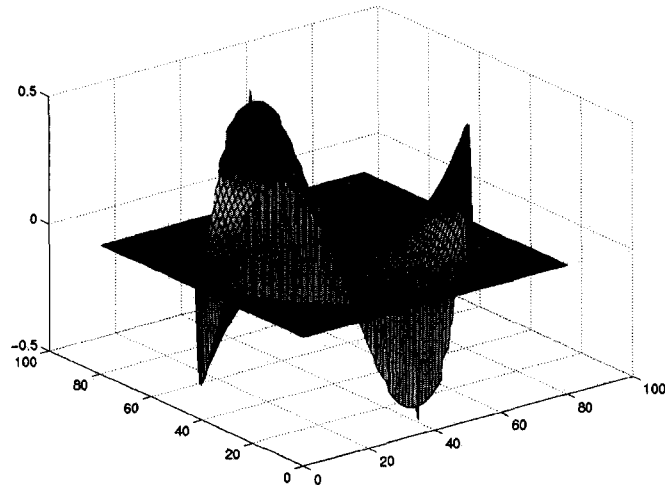
Keywords: adaptive optics, wavefront sensing, phase contrast

## 1. INTRODUCTION

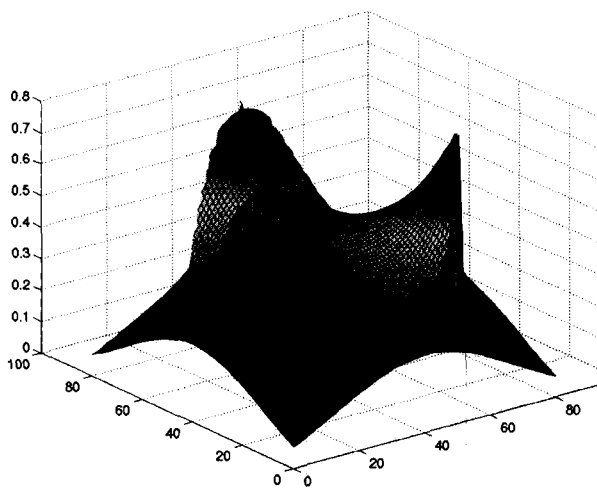
We present quantitative arguments supporting the potential usefulness of the Zernike phase-contrast technique as a real-time wavefront sensor and as a tool for calibration of non-common-path errors in adaptive optics (AO) systems. Originally developed for microscopy<sup>1</sup> as a way to render phase objects visible with good amplitude definition, the technique converts phase variations over an entrance pupil (such as a telescope aperture) into intensity variations over a re-imaged pupil by means of a phase-shifting filter inserted in an intervening focal plane. The simplest case of monochromatic operation on a telescope of diameter  $D$  requires a filter that induces an extra phase shift of  $\pi/2$  over a diffraction-limited spot size of diameter roughly  $\lambda D$ , in excess of that experienced by rays further off-axis that traverse an equal thickness of air. If the phases  $\Phi$  to be measured are small, the intensity in the re-imaged pupil is proportional to  $1+2\Phi$ , implying a "phase-contrast signal" map  $2\Phi(\xi,\eta)$  superimposed on a uniform intensity across the entire pupil.

The physics of the phase-contrast technique is described in a number of standard texts<sup>2,3</sup>. Briefly, the Fourier-optical expression for focal-plane intensity as a function of pupil phase  $\Phi(\xi,\eta)$  is  $|\text{F.T.}\{A(\xi,\eta)\exp[i\Phi(\xi,\eta)]\}|^2$ , where  $\xi$  and  $\eta$  are pupil-plane coordinates and  $\text{F.T.}\{\dots\}$  denotes the two-dimensional (spatial) Fourier transform. In the limit of small phase  $\Phi$ , the exponential may be expanded as  $1+i\Phi$ , indicating that the phase contrast signal is normally  $\pi/2$  out of phase with a uniform background over the re-imaged pupil. The uniform background over the pupil results in a diffraction-limited point-spread function (PSF) in the focal-plane intensity, of width  $\sim \lambda D$ , while the weaker term  $i\Phi$  represents power diffracted off-axis from this PSF. This separation in the focal plane allows a filter matched in size to the PSF to advance or retard the relative phase of the undiffracted central ray; when the squared modulus of  $A\exp[i\Phi]$  is subsequently evaluated in the re-imaged pupil, an intensity map proportional to  $1\pm 2\Phi$  results, to leading order in  $\Phi$ .

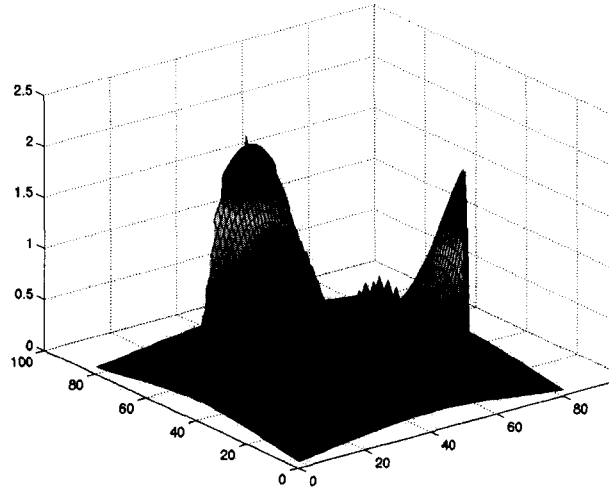
This conversion of pupil phase to intensity in the re-imaged pupil is illustrated in Figure 1, a numerical simulation of phase-contrast wavefront sensing in which the input pupil phase function is assumed to be pure trefoil with a strength equivalent to a Strehl ratio of either  $S = 0.99$  or  $S = 0.70$ . At  $S = 0.99$  the phase perturbation is small, so the small-phase approximation is a very good one; as a result, the re-imaged pupil intensity, though imposed on a uniform background intensity, is a very good replica of the input phase function. At somewhat lower Strehl,  $S = 0.70$ , more of the guide-star light is contained in the phase-contrast channel and there is less of a plateau, but the sensor output is somewhat distorted.



**Input phase function (trefoil; arbitrary units)**



**Output for  $S = 0.99$**



**Output for  $S = 0.70$**

Figure 1 – Numerical simulation of the operation of the phase-contrast wavefront sensor. The upper panel shows a test phase function imposed on the input pupil, and the lower panels show the resulting monochromatic image intensities at the reimaged pupil plane. Very small phase errors ( $S = 0.99$ , at lower left) give highly linear response: except for scale factors and a constant offset, the intensity in the reimaged pupil faithfully reproduces the input phase function. Moderate phase errors ( $S = 0.70$ , at lower right) result in a somewhat distorted response.

## 2. CURRENT WAVEFRONT SENSORS ON ASTRONOMICAL AO SYSTEMS

The vast majority of astronomical adaptive optics systems have used either Shack-Hartmann or “curvature” wavefront sensors. The curvature sensor produces an error signal proportional to the local curvature (second spatial derivative) of pupil phase, and has primarily been coupled to bimorph deformable mirrors, which in turn induce a local phase curvature response that is directly proportional to the drive signal. More common are “piston-type” deformable mirrors composed of arrays of PZT or PMN actuators that produce a local phase correction proportional to the applied drive signal. These have traditionally been coupled to Shack-Hartmann wavefront sensors, whose error signals are proportional to the first spatial derivative of phase; appropriate drive signals are derived by the wavefront reconstruction process.

Curvature sensors can be integrated into very simple and cost-effective AO systems, and have been used to great effect in a number of instruments having modest numbers of actuators<sup>4</sup>. Measurement error in a single subaperture of a curvature sensor is comparable to that in a single Shack-Hartmann subaperture<sup>5</sup>, but error propagation through the reconstruction process is worse, increasing as the logarithm of the square of the array size rather than just logarithmically as in the Shack-Hartmann wavefront sensor<sup>6</sup>. As a result, we will restrict our discussion to Shack-Hartmann wavefront sensors, the approach generally considered most promising for high adaptive correction with large actuator counts. They are also more commonly used in large astronomical adaptive optics systems, and a Shack-Hartmann is used by the system of most interest to us, the Palomar Adaptive Optics system<sup>7,8</sup>. In later sections we will compare the performance of a phase-contrast wavefront sensor to that of the Shack-Hartmann alone, as representative of the current state of the art for large astronomical AO systems.

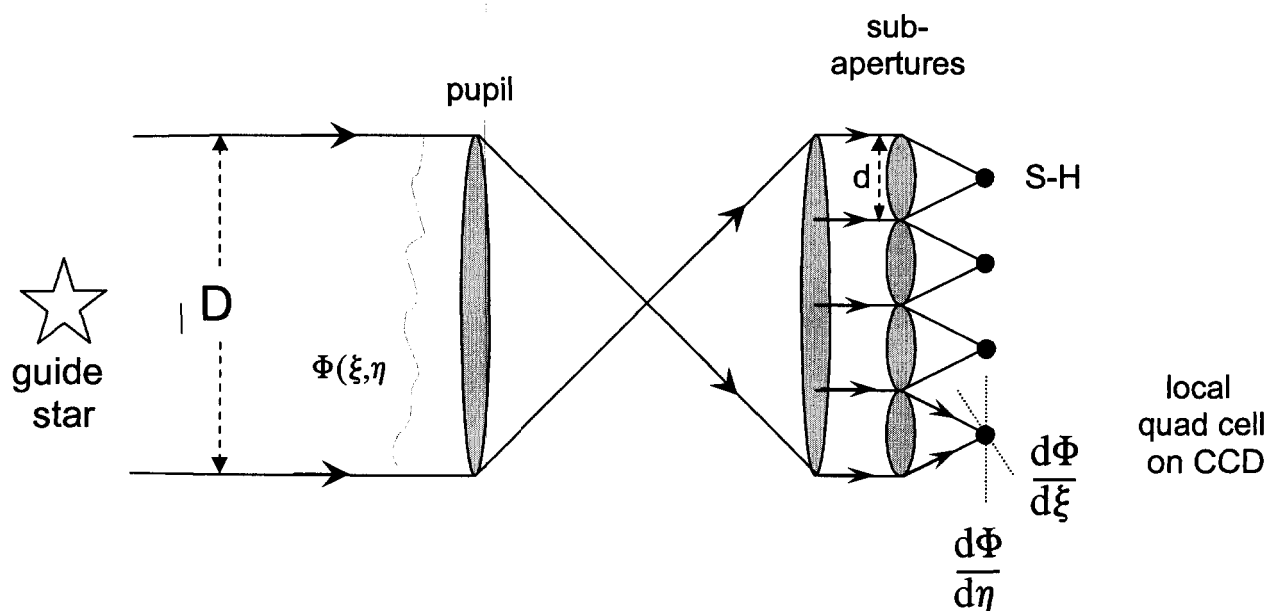


Figure 2 – Schematic of a Shack-Hartmann wavefront sensor. The CCD camera senses deflections of focal spots produced by lenslets defining equivalent subapertures  $d$  roughly matched to  $r_0$ . These deflections, sensed by groups of 4 pixels acting as quad cells, are proportional to the local phase gradients on the pupil.

### 3. CALIBRATION OF NON-COMMON-PATH ERRORS WITH THE PHASE-CONTRAST WAVEFRONT SENSOR

Another useful application of the phase contrast technique is calibration of the non-common path errors of an adaptive optics system. Figure 3 illustrates PALAO, the Palomar Adaptive Optics system (and its Shack-Hartmann wavefront sensor). Wavefront perturbations are sensed at optical wavelengths and are corrected for science observations in the near-infrared. So imperfections in the optical path downstream of the dichroic at which this wavelength division is carried out are not automatically corrected by the closed-loop action of the AO system. Such errors, which may typically be caused by drifts in positions of optical elements due to time-varying flexure, are termed “non-common-path” errors, and can impose significant limitations on system performance. One approach to dealing with them is to perform periodic calibrations by setting WFS centroids, which drive DM positions in closed loop, to optimize the PSF seen by the science camera. These calibrations can be carried out very effectively by making minor operational modifications to PALAO that allow it to operate in a phase-contrast wavefront sensing mode<sup>9</sup>.

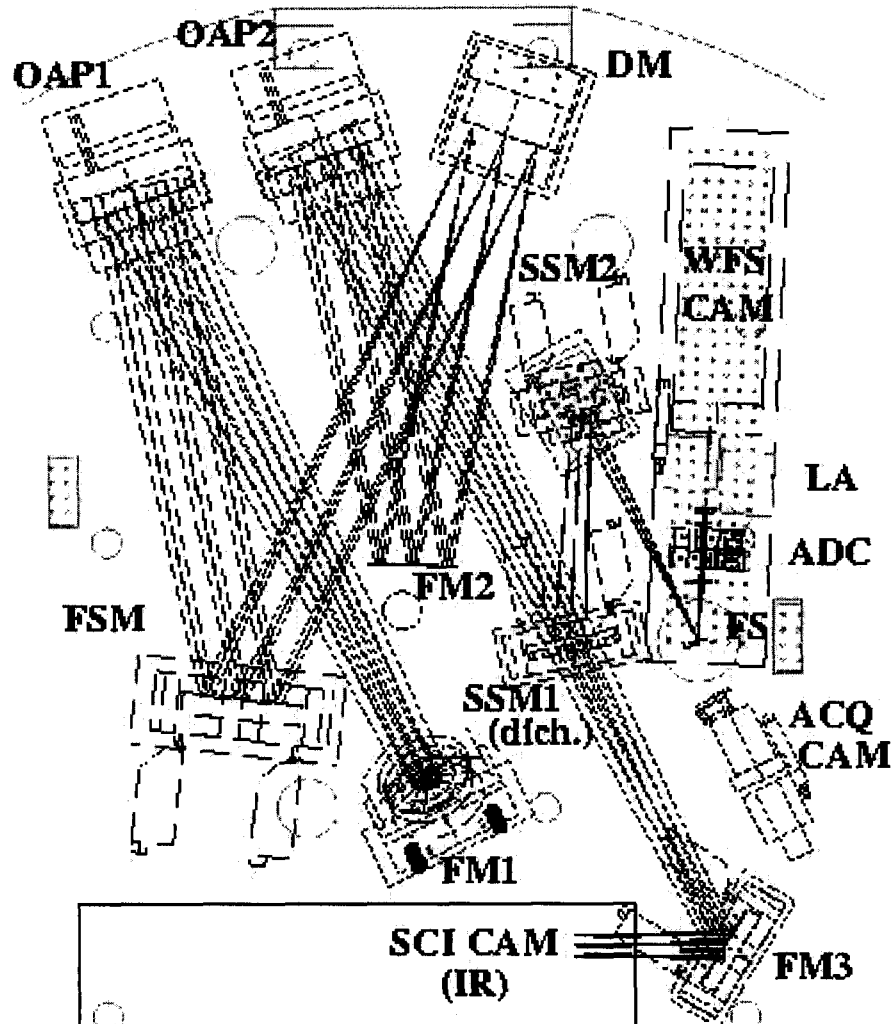


Figure 3 – Schematic of PALAO, the Palomar Adaptive Optics system, fairly typical of high-order systems using Shack-Hartmann wavefront sensors. Light from the telescope is injected at FM1. Fast tip-tilt correction is applied by FSM; higher-order correction is provided by DM. The science camera operates in the near-infrared; visible light is sent to the wavefront sensor via steering mirrors SSM1 (a dichroic) and SSM2. The reflective field stop (FS), a 4 arcsec x 4 arcsec metallization on an otherwise transparent substrate, directs the guide-star light through the Shack-Hartmann lenslet array (LA) and onto the CCD camera (WFS CAM).

A true Zernike phase-contrast mode would require a  $\pi/2$  phase-shifting filter to be added to the existing coronagraphic filter wheel located inside the science camera. This filter would be placed in the focal plane, and the pupil of the telescope/AO system would be imaged in the light of an internal white-light source built into PALAO for other calibration purposes. (The pupil imaging mode and the single mode source is an easily-selected operating mode of PHARO, PALAO's science camera, that has been provided for a number of other diagnostics.) With this configuration implementing a phase-contrast focal-plane filter, any area of the pupil image that deviates from the average intensity, either brighter or darker, will correspond to phase deviations from the average (e.g. due to surface zones on the primary mirror that are either high or low, respectively) that may be incorporated into the wavefront sensor's PSF calibration.

Unfortunately, a  $\pi/2$  phase filter is not readily available in the filter complement of any AO system. A workable substitute, however, is one of the suite of focal-plane occulting masks used in coronagraphy. Using an opaque mask of this sort, of roughly diffraction-limited diameter, yields a variant of the Zernike wavefront sensor in which the DC term (undiffracted ray) is blocked, leaving only the  $i\Phi$  term describing the higher-order, diffracted rays. In the re-imaged pupil, the intensity distribution is proportional to  $\Phi^2$ . The sign of the phase disturbance has now been lost, and auxiliary steps must be carried out to recover it; in our implementation, that is done by measuring the intensity changes for different DM positions. The procedure and experimental results for a test in which a single deformable-mirror (DM) actuator is driven to give a local phase disturbance in the pupil plane are described below.

In this test, we assume the intensity depends on phase according to:

$$I(x, y) = A (\varphi(x, y; i) - \varphi_0(x, y; i_0))^2 + C \quad (1)$$

where  $A$  and  $C$  are constants. The constant  $C$  is the DC background (or 'glow') as discussed previously. At a single pixel position  $(x, y)$ , this can be re-written as a function of DM drive signal  $i$  as:

$$I(x, y) = A' (i - i_0)^2 + C \quad (2)$$

If we take multiple images of the re-imaged pupil, each with a different value for the DM actuator position, we can solve for all three variables ( $A'$ ,  $i_0$ ,  $C$ ) using a linear least-squares algorithm.

These tests were performed with the AO instrument white-light source when the system was in the laboratory. The fold mirror in front of the science camera (FM3) was manually adjusted to center the re-imaged spot behind the 0.43" coronagraphic spot. Since the white light source pupil is ill-defined, the pupil mask was put on the front of the DM. The science camera was tilted about its focal plane in order to center the DM pupil with the internal Lyot mask (Std. Cross). We used the 'K' filter and an integration time of  $\sim 10$  seconds. At these settings, the typical intensity values were  $\sim 5400$ . The pupil images are recorded on a 1024x1024 array, and then sampled down to match the DM actuator spacing. A processed image of the pupil is shown below in Fig. 4.

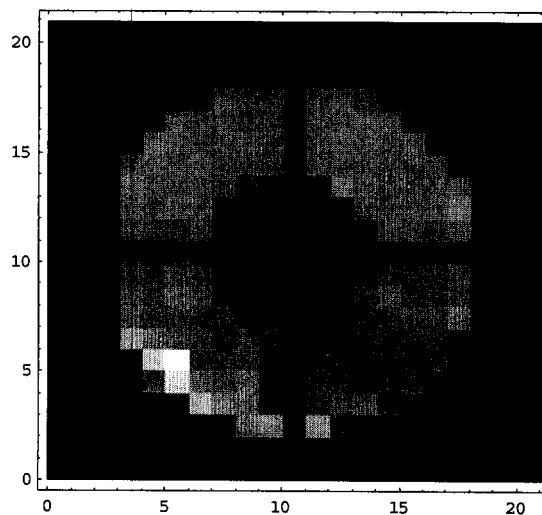


Figure 4 – Sample processed pupil image showing a 'bright' local feature in the telescope pupil, at lower left, corresponding to a local phase deviation from the average induced by commanding a single deformable-mirror actuator at (5,5).

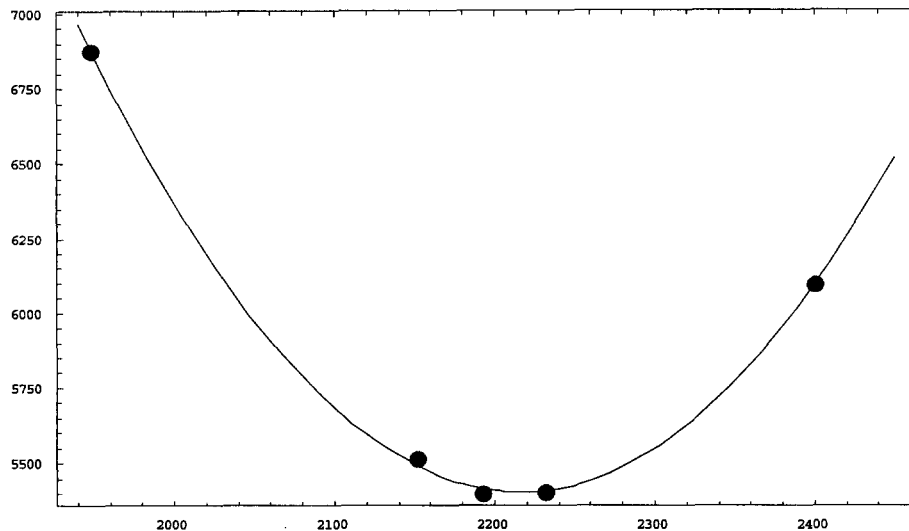


Figure 5 – Raw data for the single actuator test. Horizontal axis is phase in DM counts, and vertical axis is intensity.

Five separate images were taken: the pupil image with nominally flat DM, and then 4 images with DM actuator changed by the following counts: -244, -40, 40 and 208. Using a least-squares technique with these five data points (Figure 5), it's possible to determine the best solution for the coefficients of Equation 2 (solid curve). The best-fit coefficients were  $A' = 0.0204 \pm 0.0004$ ,  $i_0 = 2216 \pm 2$ , and  $C = 5400 \pm 10$ . The actuator we used, (5,5), started at a value of 2192, so we measured an optimum value different by 24 counts (or 0.12  $\mu\text{m}$ )

#### 4. TRADEOFFS BETWEEN PHASE-CONTRAST AND SHACK-HARTMANN REAL-TIME WAVEFRONT SENSORS

Note that, anticipating the discussion of Section 5 in which achromatization of the phase-contrast filter is presented, we do not count bandwidth as an advantage for the Shack-Hartmann wavefront sensor. However, the Shack-Hartmann is intrinsically very broad-band, if spot sizes do not exceed the linear response range of the 4-pixel quadrant detectors at each wavelength. Careful optical and thin-film designs are required to achromatize the phase-contrast wavefront sensor, and if the wavelength range of the Shack-Hartmann cannot be matched it will suffer a larger wavefront variance in inverse proportion to the ratio of bandwidths.

##### a) Disadvantages of Phase-Contrast WFS:

###### i. Incomplete Use of Guidestar Light

Only a fraction of the total guide-star light carries phase information in the phase-contrast wavefront sensor. In the small-phase approximation, the illumination of the re-imaged pupil is proportional to  $(1+2\Phi)$ , where  $\Phi$  is the phase signal, so the amount of light contains useful information drops as the image quality is improved. At a Strehl ratio  $S=0.60$ , roughly the performance limit of the Palomar adaptive optics system, and the regime in which we have considered implementing a phase-contrast wfs in a bootstrapped mode to boost the quality of the correction, the rms phase error across the pupil is  $\Phi \sim 0.6$ , so roughly 56% of the light is channeled into useful signal. At  $S=0.90$ , which would constitute substantially improved imaging, the rms phase error is  $\Phi \sim 0.3$ , implying that 39% of the guidestar light is useful for decoding phase information. So the fraction of light containing useful wfs information remains relatively high even at high degrees of image correction. Even at  $S=0.99$ , one-sixth of the guidestar light is contained in the phase-contrast channel (Figure 6).

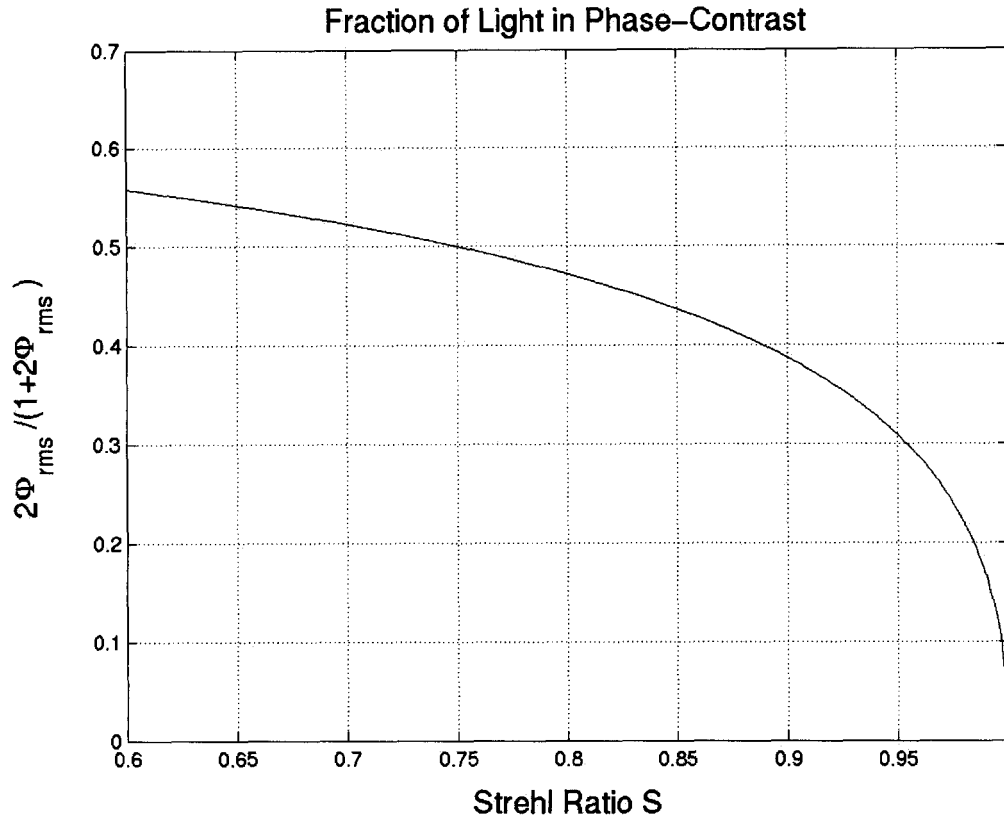


Figure 6 – Amount of guide star light appearing in phase contrast ( $2\Phi$ ), as a fraction of the total guide star light, ( $1+2\Phi$ ), at an rms residual phase level  $\Phi$  corresponding to a given Strehl ratio via the (extended) Maréchal approximation,  $\Phi = \sqrt{1-S}$ . Even at very high performance levels, a substantial fraction of guide star light in the phase contrast wavefront sensor is contained in the phase contrast channel.

## ii. Non-linear Response

The approximation used to derive the phase-contrast signal, ( $1+2\Phi$ ), depends on a linear expansion of a complex exponential, and so is strictly true only in the limit of small input phase disturbances  $\Phi \ll 1$  (that is, high Strehl ratio S). In fact, at  $S = 0.79$ , the rms phase error across the pupil is  $\Phi_{rms} = 0.55$  rad. The first neglected term in the exponential expansion is smaller by this same factor. An intuitive sense for the non-linear distortion may be had by inspection of the lower-right panel of Figure 1. Though it is possible in principle to operate in the non-linear regime of the phase-contrast wavefront sensor<sup>10</sup>, so this is not a fundamental disadvantage, analysis and wavefront reconstruction are much simpler when linearity (high S) can be assumed.

## b) Advantages of Phase-Contrast WFS:

### i. Better Error Propagation in Reconstruction:

A substantial sensitivity advantage of the phase-contrast wavefront sensor over the Shack-Hartmann wavefront sensor is lower error propagation during wavefront reconstruction, even though errors in the individual phase measurements per subaperture are comparable in the two techniques<sup>11</sup>. Qualitatively, the advantage is an extension of the main advantage that the Shack-Hartmann has over the curvature sensor: the phase gradients measured by the Shack-Hartmann are more highly correlated between adjacent subapertures, and this redundancy is exploited during reconstruction to give more benign error propagation<sup>5,11</sup>. Presumably, direct phase measurements are more correlated still.

More quantitatively, for a corrected pupil consisting of an  $N \times N$  array of subapertures, Fried<sup>12</sup> found that the error coefficient describing the ratio of mean-square error in the reconstructed wavefront to that in the one-axis single-subaperture phase in a Shack-Hartmann could be written as

$$\langle (\delta \Phi)^2 \rangle \approx 0.6558 \left[ 1 + 0.2444 \ln(N^2) \right] \sigma_{1-axis}^2 \quad (3)$$

For a wavefront sensor measuring phase differences directly, Hudgin<sup>13</sup> found the following analogous expression:

$$\langle (\delta \Phi)^2 \rangle \approx [0.561 + \ln(N)] \sigma_{1-axis}^2 \quad (4)$$

For a  $16 \times 16$  subaperture grid, as used by the Palomar adaptive optics system, the ratio of these two expressions favors phase-contrast wavefront sensing by a factor of about 1.8 in mean-square wavefront error. (For a future extreme AO system having  $100 \times 100$  subapertures, this ratio grows, but only modestly, to about 2.0.)

## ii. Simpler/Faster Computation

The natural coupling of direct-phase wavefront measurements to a piston-type deformable-mirror (DM) actuator could make reconstruction almost unnecessary, greatly simplifying and speeding up the computational load associated with the AO control loop. At present, latency caused by real-time computation is one of the limiting factors in the quality of corrected images from PALAO, particularly when guide-star light is plentiful. Full matrix reconstruction in the Shack-Hartmann case involves multiplying a  $N^2 \times 2N^2$  control matrix by a  $2N^2 \times 1$  column vector of x- and y-gradients of the pupil phase to obtain  $N^2$  updated DM actuator positions. This involves  $\sim 2N^4$  multiplication and additions. In the phase-contrast case, reconstruction would involve multiplying a square  $N^2 \times N^2$  control matrix by an  $N^2 \times 1$  column vector of pupil phases, and would involve half as many mathematical operations.

The Shack-Hartmann control matrix is the pseudo-inverse of an influence matrix that gives the wavefront sensor response (phase gradients) as a function of wavefront (DM actuator deflection). The influence matrix is relatively sparse: if the influence function of individual DM actuators is neglected, it consists of 4 non-zero diagonals representing the 4 DM actuators that determine gradients in any wavefront sensor subaperture. The control matrix pseudo-inverse is generally fully populated. However, if it can be approximated by a sparse matrix, the computational load can be reduced from  $2N^4$  to  $2d^2N^2$ , where  $d$  is the number of actuators over which the DM influence function extends. The phase-contrast influence matrix is square, and very close to diagonal, so its inverse is also close to diagonal. Thus the increased computational efficiency of sparse-matrix techniques should be much more effective. One may think of comparing the sum of the influence width  $d$  due to DM actuators with either the 4 diagonals of the Shack-Hartmann or the single diagonal of the phase-contrast wavefront sensor; this summarizes the advantages of matching a phase-piston wavefront sensor to the phase-piston DM.

*check...the PUSH/INFLUENCE matrix is sparse, but RECONSTRUCTOR/CONTROL MATRIX is not...see the example from the web... also, DOESN'T THE PH-CONT RECONSTRUCTOR RETAIN ITS DIAGONAL NATURE ON INVERSION BETTER THAN SH DOES ON PSEUDO-INVERSION? ...check this with MATLAB...*

## iii. Lower Detector Read Noise

An additional sensitivity advantage of the phase-contrast wavefront sensor over the Shack-Hartmann is that the latter requires reading out four pixels in the WFS CCD camera to make a single subaperture measurement, while the latter requires reading out just one. Although CCD cameras can in principle be made to have very low read noise, most cameras actually in use have read noise that is not totally negligible. The Palomar adaptive optics system, for example, has read noise on the order of 10 electrons at high frame rates.

## iv. Freedom from Image Artifacts (e.g. "Waffle Mode")

A familiar drawback of the Shack-Hartmann wavefront sensor when it is coupled to a square array of deformable-mirror actuators in the "Fried" geometry is the introduction of time-variable artifacts into the corrected image. The classic case consists of a square arrangement of spots of light arranged symmetrically about the PSF peak. This "waffle mode" image defect results from the fact that the Shack-Hartmann cannot sense pupil-plane phase patterns corresponding to a

checkerboard pattern of actuators alternating between two offset levels; this mode and the corresponding image-plane artifacts then tend to grow in a random-walk fashion if no special actions are taken to monitor them. No comparable defects could be incurred when phase is sensed directly by the phase-contrast wavefront sensor, because there are no pupil-plane phase modes (except for simple piston) that are not sensed by the subaperture arrangement. Hence the phase-contrast wavefront sensor enjoys a cosmetic advantage over the Shack-Hartmann when that wavefront sensor is configured in the usual “Fried” geometry.

#### v. Freedom from Centroid Anisoplanatism seen in Shack-Hartmann

Immunity from centroid anisoplanatism errors favors the phase-contrast wavefront sensor; the size of the error is small in a Shack-Hartmann operated under normal conditions, but we include it here for completeness.

The turbulent atmosphere over a subaperture of the wavefront sensor may be analyzed as a certain composition of Zernike modes that depends on the relative size of the subaperture diameter,  $d$ , and the transverse coherence scale of the turbulence,  $r_0$ . A Shack-Hartmann wavefront sensor, in measuring local tilt, will make an error because some other Zernike components contribute an intensity-weighted centroid that is not centered on the subaperture quadcell. This is sometimes referred to as the difference between G-tilt, or gradient tilt, which is measured by the Shack-Hartmann, and Z-tilt, or Zernike tilt, which is the proper tilt component of the turbulence. It is related to the fact that the Zernike phase functions are orthogonal over the pupil, but their squared moduli, or corresponding image intensities, are not. A notable low-order contribution to the centroid anisoplanatism error is made by coma, which has an asymmetric image intensity distribution that contributes a non-vanishing (and erroneous) spot displacement in a Shack-Hartmann quadcell.

Sasiela<sup>14</sup> derives the following expression for the mean-square wavefront error that would be made by a wavefront sensor measuring G-tilt, as a Shack-Hartmann does, over a subaperture of diameter  $d$ , for atmospheric turbulence having a Kolmogorov spectrum and characterized by a transverse coherence scale  $r_0$ :

$$\langle (\delta \Phi)^2 \rangle_d = 0.0061 \left( \frac{d}{r_0} \right)^{5/3} \left( \frac{\lambda}{d} \right)^2 \approx 0.0061 \left( \frac{\lambda}{d} \right)^2 \quad (5)$$

The last form assume wavefront sensor subapertures matched in size to  $r_0$ , as is usually the case. This wavefront variance is about 1% of that in true tip/tilt, so this source of error is not large for normal situations. But formally, the phase-contrast wavefront sensor is immune to this error while the Shack-Hartmann is not.

The Shack-Hartmann wavefront sensor uses essentially all of the guidestar light to measure its local derivatives of pupil phase. However, it suffers from some problems that become particularly important when a very high fidelity wavefront measurement is desired to achieve Strehl ratios higher than 0.60.

### 5. ACHROMATIZATION OF THE PHASE-CONTRAST WFS

Maximum sensitivity of any real-time wavefront sensor is critical, and it requires response to a broad wavelength band of guide star light. The Shack-Hartmann wavefront sensor is intrinsically broad-band, with a spot deflection that is nominally independent of wavelength for a given subaperture tip/tilt. Note though that the behavior of the Shack-Hartmann wavefront sensor depends on the spot size, which in turn depends on wavelength as  $\lambda/d$ . But if the Shack-Hartmann is designed correctly, so that the spots at all wavelengths avoid saturation and remain within the linear response region, this is not an issue.

Achromatization of the phase-contrast WFS may be accomplished by the combination of two distinct design modifications, one involving the phase-shifting focal-plane filter, and one involving external optics. First, the optical thickness of the phase-shifting spot should be arranged to be reasonably close to  $\pi/2$  over the range of wavelengths of interest; second, the spot should have a diffraction-limited transverse scale of roughly  $\lambda/D$ , where  $D$  is the diameter of the telescope aperture, for all wavelengths  $\lambda$  of interest. Roughly speaking, the former requirement addresses the size of the phase shift between the undiffracted wave and the higher-order waves that carry pupil-phase information, while the latter addresses the spatial extent of the undiffracted wave. Both of these requirements can be met without adding undue complexity to the wavefront sensor system, and will be discussed in detail in the next two sections.

#### **a) Achromatic Phase Shift through Focal-Plane Spot**

The problem of achromatizing the phase shift through the focal-plane spot may be solved by fairly standard techniques that are used to fabricate multi-layer films, such as anti-reflection coatings. The size of the phase-shifting filter, a diameter of about  $\lambda D \sim 25 \mu\text{m}$  at visible wavelengths, is easily within the capabilities of thermal deposition with a lift-off photolithographic process. Convenient basic building blocks are high- and low-index films that are individually durable and adhere well to each other; one such standard system would be  $\text{TiO}_2$  ( $n = 2.3$ ) and  $\text{SiO}_2$  ( $n = 1.5$ ).

The problem of fabricating a filter with an achromatic phase shift of  $\pi$  has been discussed by in the context of four-quadrant phase-mask coronagraphy<sup>15</sup>. The particular solution they propose is directly applicable to our requirements, as they achieve relative phase shifts of  $\pi$  with phase shifts of  $+\pi/2$  and  $-\pi/2$  in alternating quadrants of their focal-plane phase mask. Their approach is moreover done in reflection from a substrate, with a double pass through the phase-shifting films, which is again directly applicable to the approach that would most easily be installed on the existing PALAO system. So this aspect of the problem is theoretically well in hand.

#### **b) Achromatic Transverse Dimension of Phase-shifting Focal-Plane Filter**

The problem of achromatizing the transverse dimension of the focal plane spot, which should be  $\sim \lambda D$  over the wavelength passband of interest, is equivalent to designing an imaging system with an achromatic transverse magnification. Simple solutions to this problem have been proposed independently by Wynne<sup>16</sup> and by Roddier et al.<sup>17</sup> In the context of speckle interferometry, where the scale of the speckle pattern is wavelength dependent, Wynne devised a corrector that gives a compensating chromatic gradient of transverse magnification opposite in sign to the speckle dispersion. (The solution of Roddier et al. is similar in approach, though executed with fewer glass layers.) Wynne's design uses two triplet lenses with an air space between them.

Performance of the achromatic corrector is given by Wynne. Over the broad spectral range from 400 nm to 700 nm, the normal wavelength-dependent variation of image height in the focal plane is  $700/400 = 1.75$ . With correcting optics in place, this linear variation is reduced to a shallow parabola, roughly the same at each end of the wavelength band, and dropping about 7% in the middle. Use of such optics with a phase-shifting focal-plane spot would clearly match the core of the diffraction-limited point-spread function, previously  $\sim \lambda D$  in diameter, to the physical size of the phase-shifting spot to good accuracy over a broad range of wavelengths. This in turn would allow accurate selection of the lowest spatial order for a phase shift of  $\pi/2$  with respect to the diffracted orders.

If the correcting optics described here were to be used in a phase-shift wavefront sensor "bootstrapped" to a standard Shack-Hartmann AO system<sup>xx</sup>, they would clearly need to be included in the beam train of the Shack-Hartmann, rather than inserted "on the fly". This appears to be no serious limitation for the PALAO adaptive optics system, where the regions on both sides of the focal plane in the field stop (Figure 3) are accessible. These optics would have no adverse effect on normal Shack-Hartmann operation, and indeed the achromatic spot size might have offer some advantages in removing centroid gain effects that depend on the color of the guide star.

## **6. CONCLUSION: BOOTSTRAPPING OF PHASE-CONTRAST WFS IN PALAO**

The qualitative analytic arguments given here indicate that there may be a performance advantage to be had by using a phase-contrast wavefront sensor in place of the Shack-Hartmann sensors now commonly used in AO systems. The loss of signal from the useful phase-contrast channel is not as severe as might be thought (Section 4.a.i), and may be offset by substantial improvement in noise propagation during reconstruction. These calculations are sufficiently promising to justify more detailed modeling and experimentation.

The signal in a phase-contrast wavefront sensor is not linear in phase until the Strehl ratio is high, and there are phase-wrapping ambiguities at low Strehl. Hence it appears most straightforward to use the phase-contrast wavefront sensor as a high-performance extension of a Shack-Hartmann, which can achieve a stable lock starting from subapertures comparable in size to  $r_0$ . One could imagine performance benefits being realized above  $S=0.70$ , the approximate limit of current correction of the Palomar adaptive optics system. To achieve competitive sensitivity, the phase-contrast

wavefront sensor would have to operate over a broad spectral bandwidth, but techniques for doing this are presented in Section 5.

A simple architecture for bootstrapping a phase-contrast wavefront sensor onto the Palomar adaptive optics system has been proposed<sup>18</sup>, and is reproduced in Figure 7. The phase-shift filter would be located halfway to the edge of the 4 arcsec field stop (FS), and a commanded tip/tilt shift of the fast-steering mirror (FSM) would “insert” it in the beam and simultaneously move the spots of the Shack-Hartmann wavefront sensor from 4-pixel quadcell vertices to the approximate centers of individual pixels. The achromatic optics that correct for transverse scale of the phase-shifting focal-plane spot would be permanently installed near the field stop (FS) in Figure 3. The phase-shifting spot’s phase thickness would be made an achromatic  $\pi/2$  using the techniques outlined in section 5. The spot would be deposited on the reflecting metallization of the field stop, and positioned roughly halfway to its edge; then a rapid move of the fast-steering mirror (FSM in Figure 3) would bring the system focus onto the phase-shifting spot. The question of how adaptive lock would be maintained during this sudden shift to a new control loop is one requiring further study, and beyond the scope of the current qualitative study. The shift by the FSM will bring subaperture light spots onto individual pixels of the CCD, realizing the desired reduction of read noise.

The shift from Shack-Hartmann to phase-contrast wavefront sensing would involve the sudden implementation of a radically different control loop, and would have to be done on a timescale shorter than the adaptive cycle time of the system. Though the software engineering of the transition will require more detailed study, there appear to be no fundamental obstacles.

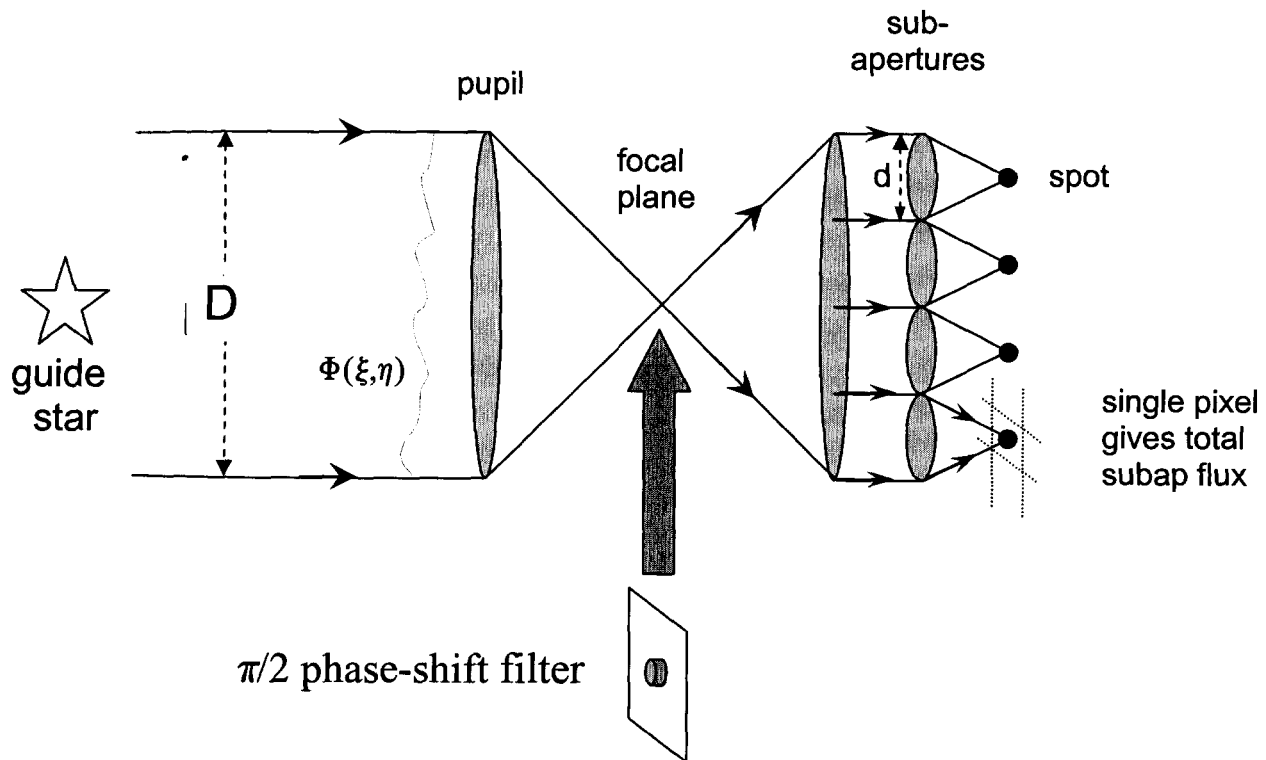


Figure 7 – Implementation of phase-contrast wavefront sensor within the optics of a Shack-Hartmann wavefront sensor, as used in PALAO, the Palomar Adaptive Optics system. The “insertion” of the phase-shifting focal-plane spot could be achieved in the Palomar adaptive optics system by a commanded shift of the fast tip-tilt correcting mirror (FSM in Figure 3), moving the subaperture intensity spots to the approximate center of single pixels in the CCD (see text).

The general considerations presented in this paper have revealed no obstacles preventing the realization of a performance boost by switching from a Shack-Hartmann to a phase-contrast wavefront sensor beyond the correction limits currently achieved by astronomical adaptive optics systems, about  $S = 0.7$  for the PALAO on the Palomar 5 m telescope. We have outlined the observational techniques for making this transition "on the fly", after a high-quality initial lock has been achieved by the Shack-Hartmann wavefront sensor. This approach appears promising, and worthy of more detailed numerical and experimental investigation. It could potentially extend the Strehl limit with relatively minor modifications to existing AO systems.

If a suitably broad-band phase-contrast wavefront sensor can be built and inserted at a high initial correction, our studies indicate that the loss in signal to the sensing channel would be roughly offset by improved error propagation through the reconstruction process, each accounting for roughly a factor of two. The largest remaining effect is substantially reduced time required to carry out the real-time reconstruction, effectively giving a substantial improvement in the closed-loop bandwidth of the adaptive control loop, and a corresponding increase in performance in the case where guide-star photons are plentiful.

## 7. ACKNOWLEDGMENTS

The research described in this publication was carried out at the Jet Propulsion Laboratory, California Institute of Technology, under a contract with the National Aeronautics and Space Administration.

## 8. REFERENCES

1. F. Zernike, "Das Phasenkontrastverfahren bei der Mikroskopischen beobachtung", *Z. Tech. Phys.*, Vol. 16, p. 454, 1935
2. J. Goodman, "Introduction to Fourier Optics", McGraw-Hill, New York, 1968
3. M. Born and E. Wolf, "Principles of Optics", Pergamon Press, Oxford, UK, 1980
4. ...some reference to a low-order but astronomically successful curvature AO system...UH? Laird Close?
5. J. W. Hardy, "Adaptive Optics for Astronomical Telescopes", Oxford University Press, New York, NY, 1998
6. F. Roddier, C. Roddier, and N. Roddier, "Curvature sensing: a new wavefront sensing method", *Proc. SPIE*, Vol. 976, pp. 203-209, 1988
7. R. G. Dekany, "The Palomar Adaptive Optics System", in *Adaptive Optics*, Vol. 13, OSA Technical Digest Series (Optical Society of America, Washington, DC), pp. 40-42, 1996
8. M. Troy, R. G. Dekany, B. R. Oppenheimer, E. E. Bloemhof, T. Trinh, F. Dekens, F. Shi, T. L. Hayward, and B. Brandl, "Palomar Adaptive Optics Project: Status and Performance", *Proc. SPIE*, Vol. 4007, pp. 31-40, 2000
9. J. K. Wallace, "Summary of phase-contrast technique as applied to DM calibration for the PalAO Science Camera", JPL Memo, 10 October 2002
10. M. A. Vorontsov, E. W. Justh, and L. A. Beresnev, "Adaptive optics with advanced phase-contrast techniques. I. High-resolution wave-front sensing", *J. Opt. Soc. Am. A.*, Vol. 18, No. 6, pp. 1289-1298, 2001
11. F. Roddier, C. Roddier, and N. Roddier, "Curvature sensing: a new wavefront sensing method", *Proc. SPIE*, Vol. 976, pp. 203-209, 1988
12. D. L. Fried, "Least-square fitting a wave-front distortion estimate to an array of phase-difference measurements", *J. Opt. Soc. Am.*, Vol. 67, No. 3, pp. 370-375, 1977
13. R. H. Hudgin, "Wave-front reconstruction for compensated imaging", *J. Opt. Soc. Am.*, Vol. 67, No. 3, pp. 375-378, 1977
14. R. J. Sasiela, "Electromagnetic Wave Propagation in Turbulence", Springer-Verlag, Berlin, 1994
15. P. Riaud, A. Boccaletti, D. Rouan, F. LeMarquis, and A. Labeyrie, "The Four-Quadrant Phase-Mask Coronagraph. II: Simulations", *Pub. Astronom. Soc. Pac.*, Vol. 113, pp. 1145-1154, 2001
16. C. G. Wynne, "Extending the Bandwidth of Speckle Interferometry", *Opt. Commun.*, Vol. 28, No. 1, pp. 21-25, 1979
17. C. Roddier, F. Roddier, F. Martin, A. Baranne, and R. Brun, "Twin-Image Holography with Spectrally Broad Light", *J. Opt. (Paris)*, Vol. 11, No. 3, pp. 149-152, 1980
18. E. E. Bloemhof and J. A. Westphal, "Design Considerations for a Novel Phase-Contrast Adaptive-Optic Wavefront Sensor", *Proc. SPIE*, Vol. 4494, pp. 363-370, 2002